



Share Your Innovations through JACS Directory

Journal of Nanoscience and Technology

Visit Journal at <http://www.jacsdirectory.com/jnst>

Synthesis, Characterization and Cytocompatibility of HfO₂ Nanoparticle Against A549 Cell Lines with Potent Antimicrobial Activities

M. Jayavel^{1,2,*}, N. Ramalakshmi¹, S. Arul Antony¹¹Department of Chemistry, Presidency College (Autonomous), Chennai – 600 005, Tamil Nadu, India.²Department of Chemistry, Meenakshi College of Engineering, Chennai – 600 078, Tamil Nadu, India.

ARTICLE DETAILS

Article history:

Received 21 July 2017

Accepted 03 August 2017

Available online 07 August 2017

Keywords:

Hafnium Oxide (HfO₂)

MTT Assay

A549 Cell Line

Nanoparticles

Precipitation Method

ABSTRACT

The rapid development of nanotechnology, the nanomaterials start to cause people's attention for potential toxic effect. In this paper the hafnium oxide nanoparticles (HfO₂ NPs) have been successfully synthesized by precipitation method using the precursors of HfCl₄ and NaOH. The synthesized materials were characterized by using X-ray diffraction (XRD), UV-visible and Transmission Electron Microscope (TEM). In addition with the cytocompatibility of Hafnium oxide nanoparticles against A549 (Human Lung Cancer Cell) cell lines was investigated. Also the synthesized compound was tested against Gram-positive and Gram-negative bacterial strains. The XRD analysis revealed the presence of monoclinic HfO₂ nanoparticles. The absorption peak at 212 nm can be assigned to absorption of HfO₂ nanoparticles. The TEM image showed that the HfO₂ NPs were of spherical in shape with particle size of about 10 nm. The Mitochondrial Toxicity Test (MTT) assay method was employed to assess cell viability after exposure to 10, 25, 50, 100 and 250 µg/mL of HfO₂ NPs for 24 h. Cell viability does not affect when the particles size at 10 nm of HfO₂ NPs and to the exposure level at 10 µg/mL. The disc diffusion method was adopted to test the antibacterial activity of HfO₂ nanoparticles exhibit better antibacterial activity for the Gram negative bacterial *K. pneumoniae* and the Gram positive bacterial *Staphylococcus aureus*.

1. Introduction

Nanomaterials are defined by the U.S. National Nanotechnology initiative as materials that have at least one dimension in the 1 nm to 100 nm range. Due to their unique physical and chemical characteristics, nanoparticles have been focus of many investigation and material applications of over the past 10 years. Several physico-chemical parameters have been proposed to be critical determinants in nanomaterial toxicity: size, crystalline structure, chemical composition, surface area, oxidation status [1] of the metal-ion.

Among all engineered nanomaterials, zirconium oxide, zinc oxide, titanium dioxide nanoparticles etc., have been extensively studied in terms of cytotoxic effects on various cell types, including macrophages, lung epithelial cells, fibroblasts of human or murin origin [2]. Though the potential effects of nanoparticles on human health remain unclear, a few preliminary studies have demonstrated toxic effects of nano-scale particles [3].

Hafnium Oxide is an inorganic compound with the chemical formula HfO₂, it can exist in three polymorphic structures, such as the monoclinic at low temperature, the tetragonal at around 2000 K and the cubic at about 2870 K [4]. Hafnium (Hf) is known as the "little brother" of titanium and zirconium. It has a large band gap (Eg: >5 eV), a high dielectric constant (εr= 25), a high material density (9.6 g/cm³), a high melting point (over 2973 K) and chemical inertness [5-9].

The toxic effects of TiO₂ NPs can be attributed to their large surface area and small size, thus increasing chemical reactivity and penetration in the living cells. TiO₂ NPs could enter the human body and injure many organs including the lung, liver, kidney, spleen, and brain [10-15].

Nanoparticles of many materials are used to enhance the radio sensitization in cancer cells such as metal based nanoparticles (gold, gadolinium, silver, titanium and hafnium), quantum dots, super paramagnetic iron oxides, non-metal based nanoparticles [16]. Maggiorella [17] have reported that, hafnium oxide NPs can acts as the best radio sensitizers to increase the dose and efficacy of radiotherapy

inside the tumor without causing any damage to surrounding healthy tissues.

The cell viability of TiO₂ on lung cells was much studied. TiO₂ was related to the generation of intracellular reactive oxygen species (ROS) and mitochondrial injury in A549 cells [18]. A549, a widely used cell system for pulmonary toxicity studies, was selected in the present study as an in vivo model to examine the cytocompatibility of HfO₂ NPs by using Mitochondrial Toxicity Test assay.

In the present study we have adopted for the precipitation method to synthesize the HfO₂ NPs and examined the cytocompatibility of synthesized HfO₂ NPs with A549 cell lines by using MTT assay. To the best of our knowledge this report is the first of its kind to study cytocompatibility of HfO₂ NPs with A549 cell lines.

Antibacterial agents kill the bacterial and inhibit their growth in the infected area and do not harm the healthier tissues. Hajipour et al [19] have been reported that the physiochemical properties of the NPs and the type of bacteria are the two important factors that determine the antibacterial activities of NPs. Azam et al [20-21] reported that CuO nanoparticles act as good antibacterial agent against *B. subtilis* and *S. aureus*. Zhou et al [22] reported Gold and silver nanoparticles display excellent antibacterial potential for the Gram-negative bacteria *E. coli* and the Gram positive bacteria. Siqueria et al [23] said that the carboxy methylcellulose film embedded with silver nanoparticles showed the best antimicrobial effect against Gram positive (*E. faecalis*) and Gram-negative (*E. coli*) bacteria. Dhanalakshmi et al [24] reported that the core-shell nanoparticles of Ag@TiO₂ and Ag@SiO₂ showed good antibacterial properties against *E. coli* and *S. aureus*. Antimicrobial activities of HfO₂, if any are an added advantage to employ the same in biological applications. Realizing this, we tested their antibacterial activities against Gram-positive bacterial strains such as *S. aureus* and *Bacillus subtilis* and Gram-negative such as *K. pneumoniae* and *E. coli*.

2. Experimental Methods

2.1 Materials

Hafnium tetrachloride (HfCl₄) was obtained from Sigma-Aldrich, Sweden. Sodium hydroxide (NaOH) was obtained from Dae Jung

*Corresponding Author

Email Address: emjayavel@gmail.com (M. Jayavel)

Chemicals, South Korea. All the chemicals used in the experiment were of research purity and were used without further purification.

2.2 Synthesis of Hafnium Oxide Nanoparticles

The HfO₂ NPs were synthesized by precipitation method using hafnium tetrachloride (HfCl₄) and sodium hydroxide (NaOH) as precursor materials. Initially, 0.4 M (100 mL) aqueous solution of NaOH was slowly added drop wise into 0.1 M (100 mL) aqueous solution of HfCl₄ and subjected to continuous stirring using teflon coated magnetic bar for 24 h, which gives a white colored precipitate containing hafnium hydroxide. The Hf(OH)₄ precipitate was washed thoroughly with Millipore water and centrifuged at 2000 rpm for 10 minutes to remove the residuals. This process was repeated many times until the precipitate was free from any trace impurities. Finally, the obtained product was dried in a hot air oven at 100 °C for 24 h and further calcined at 800 °C for 4 h which results in the formation of HfO₂ NPs.

2.3 Characterization of HfO₂ NPs

The crystal structure, orientation and crystalline size of the HfO₂ NPs were examined by Rigaku X-ray diffractometer using Cu K_α (λ = 1.5406 Å) radiation. The optical absorption spectrum of HfO₂ NPs was recorded using a UV-Vis spectrophotometer (Hewlett Packard HP-8453). The surface morphology and particle size of HfO₂ NPs were evaluated by high resolution transmission electron microscopy operated maximum acceleration voltage of 120 kV (Hitachi H-7650, Singapore).

2.4 Cell Viability

The viability of A549 cells treated with different concentrations of TiO₂ NPs was determined by MTT assay [25]. In this present investigation the synthesized HfO₂ NPs was examined by MTT assay to evaluate the possible cytocompatibility of the test samples. A549 cells were plated on 96-well plates with 5 × 10³ cells in 100 μL medium per well. Then, the plates were incubated at 37 °C for 24 h.

Then, different concentrations of HfO₂ NPs (10, 25, 50, 100 and 250 μg/mL) were added to the wells, and the culture was further incubated for 24 h. Complete medium was used as a negative control in all cases. Culture medium without the HfO₂ NPs served as the control in each experiment. After this treatment, aliquots of 10 μL MTT in Dulbecco's Phosphate Buffered Saline (DPBS) were added to each well into a final concentration of 5 mg/mL in the 96-well plates. Afterwards, the plates were incubated for another 4 h at 310 K and filtered. Subsequently, the culture medium was removed carefully, and the plates were washed carefully twice with DPBS buffer. Then, aliquots of 100 μL of DMSO were added into each well and oscillated until the formazan crystals were dissolved completely. The mixture was measured at 570 nm using a microplate spectrophotometer (ELISA 800, BioTek, USA).

2.5 Morphologic Observation

A549 cells (5 × 10³ cells/mL) were seeded on the coverslips in six-well plates and treated with HfO₂ NPs at different concentrations (10, 25, 50, 100 and 250 μg/mL) for 24 h. The changes in cell morphology were observed using inverted fluorescence microscope (AMG EVOS fl, USA).

2.6 Antibacterial Activity of HfO₂ NPs

The disc method was followed to test the antimicrobial activity of the synthesized HfO₂ NPs. Since factors, such as pH, composition of the medium, diffusion of the species and inoculum concentration can influence the size of the zone of inhibition, stringent standardization was maintained. A known weight of synthesized NPs, 10 μg, 100 μg and 1000 μg were dissolved in a minimum quantity of DMSO and it was impregnated in a sterile filter paper disc of size 4 mm. It was then allowed to dry. The disc, dipped only in DMSO after drying was used as the control. The plates, containing nutrient agar were used and seeded with different organisms at concentrations of 2 × 10⁷-3 × 10⁷ in colony forming unit (CFU) using sterile swab. The discs containing the sample were placed at different positions fine pointed forceps. The plates were incubated at 37 °C for 24 h, followed by measuring the zones of inhibition. The observations were made under sterile condition.

3. Results and Discussion

3.1 X-Ray Diffraction Study

The orientation and crystallite size of the HfO₂ NPs were investigated by X-ray diffraction (XRD) pattern. The Fig. 1 shows a typical XRD pattern of the HfO₂ nanoparticle annealed at 1073 K.

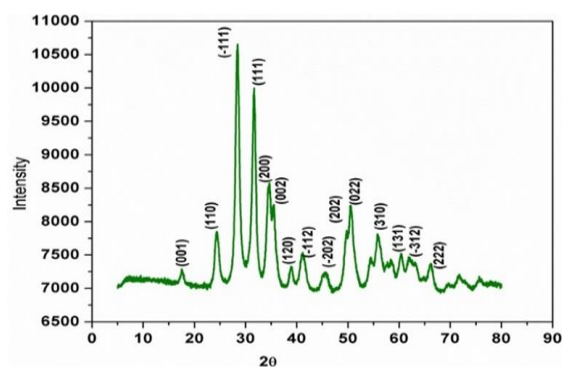


Fig. 1 X-ray diffraction pattern of HfO₂ nanoparticles

From the XRD pattern, it was found that the synthesized HfO₂ NPs have monoclinic structure with the preferential orientation of (-111) plane at 2θ = 28°, which denotes it is equivalent with the respective Joint Committee on Powder Diffraction Standards (JCDPS) No. 34-0104. The other major characteristics peaks found at 24°, 28°, 31°, 34°, 35°, 49°, 50°, 55° on the 2θ scale corresponds to the (110), (-111), (111), (200), (002), (202), (022), (310) planes respectively. Subramanian [26] have reported the particle size of synthesized NPs were calculated using a Debye - Scherrer's formula.

$$D = \frac{0.9\lambda}{\beta \cos\theta} \quad (1)$$

where D is the particle size, λ is the X-ray wavelength (1.54 Å), β is the full width half maximum) and θ is the Bragg diffraction angle. Using the Eq. (1), the particle size was found to be 10 nm.

3.2 Optical Properties of the HfO₂ NPs

The optical properties of HfO₂ NPs were studied by UV-vis absorption spectroscopy. The UV-Vis absorption spectrum of the HfO₂ NPs is shown in Fig. 2.

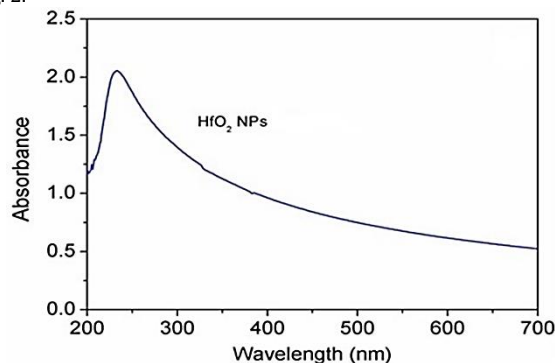


Fig. 2 UV-Visible absorption spectra of HfO₂ NPs

Takeuchi [27] have been reported the absorption peak at 210 nm corresponds to the absorption of HfO₂ NPs. In our study, the absorption of HfO₂ NPs found at 212 nm.

3.3 Morphology of the HfO₂ NPs

The surface morphology of the synthesized HfO₂ NPs have been investigated by Transmission Electron Microscope (TEM) analysis. TEM image and its SAED pattern of HfO₂ NPs were shown in Fig. 3.

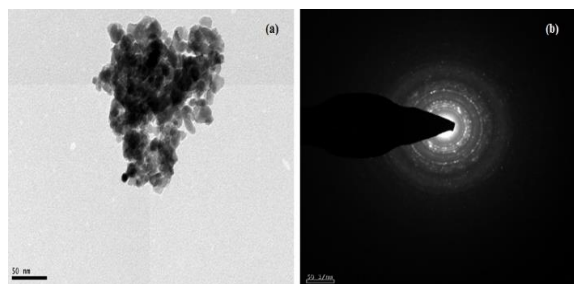


Fig. 3 (a)HR-TEM images of HfO₂ nanoparticles (b)its corresponding SAED pattern

From the Fig. 3(a), it is clearly shows that the particles are found to be spherical in shape and a small agglomeration was observed. This is due to the high surface interaction between nanoparticles which have large specific area and high surface energy. From the TEM analysis, it was found that the particles size of NPs were 10 nm. The Fig. 3(b) shows the Selected Area Electron Diffraction (SAED) pattern of HfO₂ NPs. SAED pattern reveals that, the diffraction rings has several spots, which confirms that the synthesized NPs were, polycrystalline in nature.

3.4 EDAX Spectroscopy

In order to prove the nature of the synthesized compounds the EDAX spectroscopy has been performed. The Fig. 4 illustrate the EDAX spectrum of HfO₂ NPs.

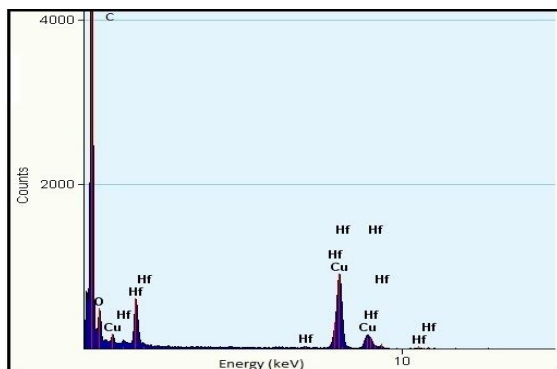


Fig. 4 EDAX spectrum of HfO₂ nanoparticles

According to EDAX measurements the synthesized NPs have been pure HfO₂, which is observed at Fig. 4. This spectrum consist of elements such as hafnium, oxygen, copper and carbon. The Hafnium and oxygen elements originated from HfO₂ NPs and carbon and copper were contributed by the carbon coated copper TEM grid.

3.5 Cytocompatibility

Since nanoparticles today are more often used in multivarious medical applications, there is an increased risk due to its size, interaction mechanism under biological condition. The main aim of this investigation was to examine the cytocompatibility of HfO₂ NPs with A549 cell lines to facilitate it for in vivo applications.

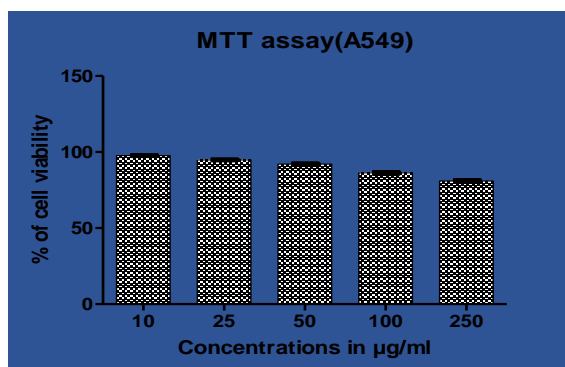


Fig. 5 Toxicity of HfO₂ NPs A549 cell lines were exposure to elevated concentration of HfO₂-NPs for 24 hours

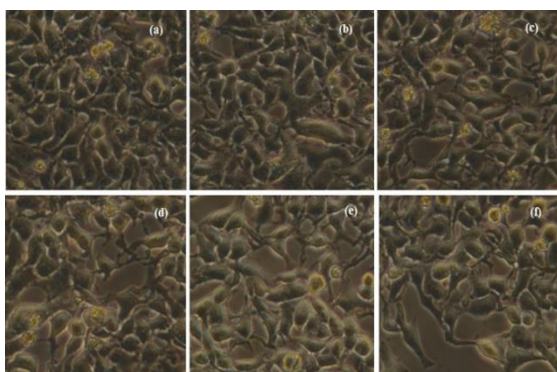


Fig. 6 Toxicity of HfO₂-NPs. (a) Control A549 cell lines, (b)-(f) (10, 25, 50, 100 and 250 µg/mL) HfO₂ NPs treated cell for 24 hours

To determine whether HfO₂ NPs are safe for human cells, we have performed a MTT (Mitochondrial Toxicity Test) assay using A549 cell lines to calculate the cell viability. The Figs. 5 and 6 illustrate the percentage of cell viability have been investigated for the synthesized HfO₂ NPs by varying the concentrations (10, 25, 50, 100 and 250 µg/mL) with A549 cell lines.

Weisheng [28] have been reported cell viability decreased from 88% to 53.9% as a function of 20 nm CeO₂ NPs concentration. In our study, the cell viability decreased from 98.50% to 82.19%, it indicates when the cells were treated with 10 µg/mL of 10 nm HfO₂ NPs the cell viability was not affected. However, with increased concentrations of HfO₂ NPs, they showed a little decrease in cell viability. Our result shows that the smaller particle has less toxicity than larger particles with A549 cell lines.

3.6 Antibacterial Activity

In this study, the antibacterial activity of HfO₂ nanoparticles was examined against two Gram-positive and two Gram-negative bacteria such as *B. subtilis*, *S. aureus*, *E. coli* and *K. pneumoniae*. The antibacterial activity results are presented in Table 1.

Table 1 Antibacterial activity of Hafnium Oxide (HfO₂) nanoparticles against two gram-positive and two gram-negative bacteria

Treatment (µg/mL)	Zone of inhibition (mm)			
	<i>E. Coli</i>	<i>B. Subtilis</i>	<i>S. Aureus</i>	<i>K. Pneumoniae</i>
10	-	-	-	-
100	8	-	9	10
1000	11	-	13	14
Ciprofloxacin	19	22	20	24

At very low concentration (10 µg/mL), all the considered pathogens did not show any zone of inhibition, whereas at concentration (100 µg/mL), HfO₂ nanoparticles exhibited maximum 10 mm zone of inhibition against *K. pneumoniae* due to diffusion of nanoparticles on nutrient agar plates. In the case of *S. aureus* and the *E. coli*, the zones inhibition were found to be 9 mm and 8 mm respectively. In contrast, the *B. subtilis* did not show any zone of inhibition. But, at higher concentration of 1000 µg/mL, the zones of inhibition were found to be of 14 mm, 13 mm and 11 mm for *K. pneumoniae*, *S. aureus* and *E. coli* respectively. In contrast, the *B. subtilis* did not show any zone of inhibition even at such higher concentration. It is clear from Table 1, that HfO₂ nanoparticles have shown greater antimicrobial activity against *K. pneumoniae*, and *S. aureus*. In another experiment, we analyzed the minimum inhibitory concentration (MIC) of HfO₂ NPs against both Gram-positive and Gram-negative bacterial strains shown in Table 2. The minimum inhibitory concentration (MIC), is the lowest concentration of material, which inhibits bacterial growth. The MIC pattern of our synthesized NPs against both Gram-negative and Gram-positive bacterial strains was found to be 89.12 µg/mL (*S. aureus*), 72.1 µg/mL (*K. pneumoniae*), 43.2 µg/mL (*E. coli*) and no value was obtained for *B. subtilis*. Since antimicrobial activity increased with the increase in surface-to-volume ratio due to a decrease in particle size of NPs, it may be expected that the smaller sized HfO₂ nanoparticles can act as good antimicrobial agents. Further to conclude, it was observed that the HfO₂ nanoparticles showed antibacterial activity against *K. pneumoniae* and *S. aureus*, little activity for *E. coli* and no activity for *B. subtilis*.

Table 2 MIC of Hafnium oxide nanoparticles against bacterial strains

Microorganisms	MIC in µg/mL	Ciprofloxacin in µg/mL
<i>E. coli</i>	43.2	12.0
<i>B. subtilis</i>	-	21.0
<i>S. aureus</i>	89.12	19.0
<i>K. pneumoniae</i>	72.1	14.0

4. Conclusion

In conclusion, HfO₂ NPs were synthesized by the precipitation method. The UV-Visible absorption spectrum showed that the absorption of HfO₂ NPs was observed at 212 nm. The XRD indicates that the synthesized HfO₂ NPs have the monoclinic crystalline in nature. TEM morphology reveals that the particle size was 10 nm, which is consistent with XRD results. In addition to this, the cytocompatibility of the HfO₂ NPs, we examined against A549 cell lines. There is no cell damage at lower concentration (10 µg/mL) of the HfO₂ NPs. The 10 nm size of HfO₂ NPs had less toxicity on interaction with A549 cell lines and can be proposed for further cytocompatibility with another cancer cell lines. The antimicrobial study has demonstrated that HfO₂ nanoparticles exhibit better antibacterial activity for the Gram-negative bacteria *K. pneumoniae* and the Gram-positive bacteria *S. aureus*.

Acknowledgement

We thank Pondicherry Centre for Biological Sciences for technical assistance with A549 cell lines and antibacterial activity.

References

- [1] S. Lanone, J. Boczkowski, Biomedical applications and potential health risks of nanomaterials, *Mol. Mech. Curr. Mol. Med.* 6 (2006) 651-663.
- [2] L.K. Limbach, P. Wick, P. Manser, R.N. Grass, A. Bruinink, et al, Exposure of engineered nanoparticles to human lung epithelial cells: influence of chemical composition and catalytic activity on oxidative stress, *Environ. Sci. Technol.* 41 (2007) 4158-4163.
- [3] E. Bermudez, J.B Mangum, B.A. Wong, B. Asgharian, P.M. Hext, et al, Pulmonary responses of mice, rats, and hamsters to subchronic inhalation of ultrafine titanium dioxide particles, *Toxicol. Sci.* 77 (2004) 347-357.
- [4] R. Terki, G. Bertrand, H. Aourag, C. Coddet, Cubic-to-tetragonal phase transition of HfO₂ from computational study, *Mater. Lett.* 62 (2008) 1484-1486.
- [5] J. Robertson, High dielectric constant gate oxides for metal oxide Si transistors, *Rep. Prog. Phys.* 69 (2006) 327-331.
- [6] G.D. Wilk, R.M. Wallace, J.M. Anthony, High-kappa gate dielectrics: current status and materials properties considerations, *J. Appl. Phys.* 89 (2001) 5243-5255.
- [7] A.A. Rastorguev, V.I. Belyi, T.P. Smirnova, L.V. Yakovkina, M.V. Zamoryanskaya, et al, Luminescence of intrinsic and extrinsic defects in hafnium oxide films, *Phys. Rev. B.* 76 (2007) 235315-235320.
- [8] S. Lance, V. Kiisk, J. Aarik, M. Kirm, I. Sildos, Luminescence of ZrO₂ and HfO₂ thin films implanted with Eu and Er ions, *Phys. Status. Solid C* 4 (2007) 938-941.
- [9] S. Lange, V. Kiisk, V. Reedo, M. Kirm, J. Aarik, et al, Luminescence of Re-ions in HfO₂ thin films and some possible applications, *Opt. Mater.* 28 (2006) 1238-1242.
- [10] G. Oberdörster, Z. Sharp, V. Atudorei, A. Elder, R. Gelein, et al, Translocation of inhaled ultrafine particles to the brain, *Inhal. Toxicol.* 6 (2004) 437-445.
- [11] H.W. Chen, S.F. Su, C.T. Chien, W.H. Lin, S.L. Yu, et al, Titanium dioxide nanoparticles induce emphysema-like lung injury in mice, *FASEB J.* 20(13) (2006) 2393-2395.
- [12] N. Li, Y. Duan, M. Hong, L. Zheng, M. Fei, et al, Spleen injury and apoptotic pathway in mice caused by titanium dioxide nanoparticles, *Toxicol. Lett.* 195(2-3) (2010) 161-168.
- [13] Z.N. Gheshlaghi, G.H. Riazi, S. Ahmadian, M. Ghafari, R. Mahinpour, Toxicity and interaction of titanium dioxide nanoparticles with microtubule protein, *Acta. Biochim. Biophys. Sin (Shanghai)* 40(9) (2008) 777-782.
- [14] J.J. Wang, B.J.S. Sanderson, H. Wang, Cyto- and genotoxicity of ultrafine TiO₂ particles in cultured human lymphoblastoid cells, *Mutat. Res.* 628(2) (2007) 99-106.
- [15] R. Meena, R. Paulraj, Toxicity. Oxidative stress mediated cytotoxicity of TiO₂ nano anatase in liver and kidney of Wistar rat, *Environ. Chem.* 94(1) (2012) 146-163.
- [16] D. Kwatra, A. Venugopal, S. Anant, Nanoparticles in radiation therapy: a summary of various approaches to enhance radio sensitization in cancer, *Transl. Cancer Res.* 2 (2013) 330-342.
- [17] L. Maggiorrella, G. Barouch, C. Devaux, A. Pottier, G. Deutsch, et al, Nanoscale radiotherapy with hafnium oxide nanoparticles, *Future Oncol.* 8 (2012) 1167-1181.
- [18] Y. Tang, F.D. Wang, C. Jin, H. Liang, X. Zhong, et al, Mitochondrial injury induced by nanosized titanium dioxide in A549 cells and rats, *Environ. Environ. Toxicol. Pharmacol.* 36 (1) (2013) 66-72.
- [19] M.J. Hajipour, K.M. Fromm, A.A. Ashkarran, D.J. de Aberasturi, I.R. de Larramendi, et al, Antibacterial properties of nanoparticles, *Trends Biotechnol.* 30 (10) (2012) 499-511.
- [20] A. Azam, A.S. Ahmed, M. Oves, M.S. Kahn, A. Memic, Size dependent antimicrobial properties of CuO nanoparticles against gram-positive and gram-negative bacterial strains, *Int. J. Nanomed.* 7 (2012) 3527-3535.
- [21] A. Azam, A.S. Ahmed, M. Oves, M.S. Khan, S.S. Habib, et al, Antimicrobial activity of metal oxide nanoparticles against gram-positive and gram-negative bacteria, a comparative study, *Int. J. Nanomed.* 7 (2012) 6003-6009.
- [22] Y. Zhou, Y. Kong, S. Kundu, J.D. Cirillo, H. Liang, Antibacterial activities of gold and silver nanoparticles against *Escherichia coli* and *Bacillus Calmette-Guérin*, *J. Nanobiotechnol.* 10 (2012) 10-19.
- [23] M.C. Siqueira, G.F. Coelho, M.R. de Moura, J.D. Bresolin, S.Z. Hubinger, et al, Evaluation of antimicrobial activity of silver nanoparticles for carboxymethylcellulose film applications in food packaging, *J. Nanosci. Nanotechnol.* 14(7) (2012) 5512-5517.
- [24] K.I. Dhanalakshmi, K.S. Meena, Comparison of antibacterial activities of Ag@TiO₂ and Ag@SiO₂ core-shell nanoparticles, *Spectrochim. Acta A Mol. Biomol. Spect.* 128 (2014) 887-890.
- [25] S.C. Liu, L.J. Xu, T. Zhang, G.G. Ren, Z. Yang, Oxidative stress and apoptosis induced by nanosized titanium dioxide in PC12 cells, *Toxicol.* 267(1-3) (2010) 172-177.
- [26] B. Subramanian, R. Ananthakumar, V.S. Vidhya, M. Jayachandran, Influence of substrate temperature on the materials properties of reactive DC magnetron sputtered Ti/TiN multilayered thin films, *Mat. Sci. Engg. B.* 176 (2011) 1-7.
- [27] H. Takeuchi, D. Ha, T.J. King, Observation of bulk HfO₂ defects by spectroscopic ellipsometry, *J. Vacuum Sci. Technol. A.* 22 (2004) 1337-1341.
- [28] L. Wisheng, Y.W. Huang, X.D. Zhou, M. Yinga, Toxicity of cerium oxide nanoparticles in human lung cancer cells, *Int. J. Toxicol.* 25 (2006) 451-457.